Crustal Magnetic Field Advection on Mars by Ionospheric Plasma Flow

I. de Oliveira[1,2], M. Fränz[2], A. Franco[1], and E. Echer[1]

[1] National Institute for Space Research, São José dos Campos, Brazil

[2] Max-Planck-Institute for Solar System Research, Göttingen, Germany

Corresponding author: Isabela de Oliveira (isabela.martins@inpe.br)

Key Points:

- Crustal magnetic field of Mars
- Ionosphere flow
- Movement of magnetic field lines

Abstract

The plasma environment of Mars is highly influenced by crustal remnant magnetism in the planet. In this work, we do statistical analyses of MAVEN and MGS data to study whether the ionospheric plasma flow can move crustal magnetic field lines, by advection. Due to the day-to-night flow of the plasma, the magnetic field lines are expected to be dragged away in anti-solar direction, causing a shift between observed and modeled field. The results show that a small shift can be observed above weak anomalies on the Northern hemisphere, where the ionospheric plasma flow is less perturbed by strong magnetic fields. To investigate the relative forces between the moving plasma and the crustal field, we also calculated dynamic, magnetic and thermal pressures, since they are involved in the advection process. In general, the dynamic pressure is lower than the other two, but this does not mean advection cannot occur, because the process is not simply a pressure balance, but a diffusive process. The calculation shows that, if advection occurs on Mars, the speed at which the crustal field lines are displaced is much smaller than the speed of the ionospheric plasma flow.

1 Introduction

In our Solar System, the interaction between the solar wind and the planetary bodies creates a region called the magnetosphere. Around planets that have an atmosphere, but do not present an active magnetic field, like Mars and Venus, an induced magnetosphere is generated (Kivelson & Bagenal, 1997; Luhmann, 1995; Luhmann et al., 1992, 2004; Podgorny et al., 1980). The solar wind interacts with the planet's ionosphere, a conductive layer which is ionized by solar radiation, especially by the extreme ultraviolet and X-rays.

Unlike Venus, the plasma environment of Mars is highly influenced by the existence of crustal remnant magnetism in the planet (Acuña et al., 1998). Above regions of intense magnetic moment, mainly located in the Southern hemisphere, mini-magnetospheres with extensions up to ~1000 km can be formed (Mitchell et al., 2001). These magnetic fields rotate with the planet, making its influence quite complicated (Brain, 2006).

It is known that the crustal magnetic fields can interfere with the processes involving atmosphere ionization and ionospheric current systems (Brain et al., 2003; Ma et al., 2002). However, we do not know whether or not the ionospheric parameters, as velocity and density, could also cause changes in the mini-magnetospheres.

In this work, we study whether the ionospheric plasma flow can move crustal magnetic field lines, by advection. The process of advection is defined as the movement of some material or field by the velocity of a fluid (Gresho & Sani, 2000). According to this hypothesis, the magnetic field lines are dragged away in the anti-solar direction, westward at dawn-side and eastward at dusk-side, as shown in Figure 1, due to the day-to-night flow of the ionospheric plasma.

The plasma flow is generally tail-ward across the complete terminator, but since crustal fields are usually mapped in latitude and longitude, we illustrate the possible effect in dawn-side and dusk-side hemispheres. The altitude range of interest is between 200 km and 1000 km. A related process is the detachment of magnetic flux ropes created by the deformation of crustal field structures, discussed by Brain et al. (2010). However, this process is beyond the scope of this paper.

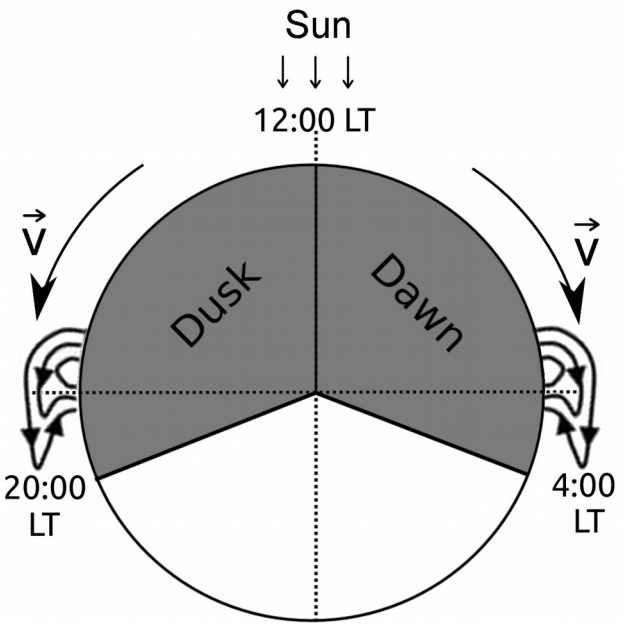

Figure 1. Schematic drawing of Mars in the XY plane (MSO coordinates), illustrating the advection process in the terminator region. The red area shows the local time (LT) coverage from MAVEN data used in this work (see Section 2).

The present work is organized as follows. In section 2, we present the data and the instruments used in the study. Section 3 contemplates the techniques used to address the problem and their respective results. In section 4, we discuss the obtained results and, in section 5, the major conclusions of this study are summarized.

2 Data and Instruments

The data used in this work were obtained by the NASA spacecrafts Mars Global Surveyor (MGS) and Mars Atmosphere and Volatile Evolution (MAVEN). We used MGS magnetic field data from the magnetometer and electron reflectometer instruments (MAG/ER) from June 1999 to November 2006, when the mission was in its Mapping Phase Orbit, which means the spacecraft was flying at a nearly constant altitude of 400 km (Acuña et al., 1992; Albee et al., 2001). MGS data sets have a high spatial coverage in areographic coordinates, although they mostly only cover the local times (LT) 02:00 LT and 14:00 LT, due to the spacecraft Sun-synchronous orbit.

MAVEN data from October 2014 to November 2018 were also used in this study. MAVEN has a sparser spatial coverage than MGS. However, the data are well distributed in local time and have an altitude range of 150 km up to 6200 km (Jakosky et al., 2015).

Magnetic field data is provided by the magnetometer (MAG) onboard MAVEN (Connerney et al., 2015). Density, temperature and velocity data of ionospheric ions are provided by the SupraThermal And Thermal Ion Composition (STATIC) instrument (McFadden et al., 2015). Here, we use the same data processing as described in Dubinin et al. (2017). Density and temperature of ionospheric electrons are obtained by Langmuir Probe and Waves (LPW) instrument (Andersson et al., 2015).

3 Techniques for Observation of the Advection Process

In this work, we investigate the hypothesis of the advection of Mars crustal fields by ionospheric plasma flow using two different methods. These are the shifting technique and the analysis of pressures, explained in the next subsections.

Another approach would be to solve the transport equation, derived by the theory of magneto-hydrodynamics (e.g., Bittencourt, 1995):

$$\frac{\partial \boldsymbol{B}}{\partial t} = \nabla \times (v \times \boldsymbol{B}) + \eta \nabla^2 \boldsymbol{B} \quad , \tag{1}$$

where $\boldsymbol{B}$ is the magnetic field vector, v is the plasma horizontal velocity and η is the magnetic diffusivity.

In physical terms, this equation means that the changes of magnetic field lines in time occur due to its advection by the plasma velocity (first term on the right-side) and its diffusion through the plasma (second term on the right-side), which is intimately related to the electric conductivity of the plasma, by:

$$\eta = \frac{1}{\mu_0 \sigma_0} \quad , \tag{2}$$

where μ_0 is the permeability of free space and σ_0 is the magnetic conductivity of the plasma. The conductivity of the Martian ionosphere cannot be directly measured and its derivation is not straightforward. Thus, the equation of motion of magnetic field lines has a higher degree of complexity to solve and it was not applied here.

3.1. Shifting Technique

The first technique is a direct comparison between magnetic field data and a crustal magnetic field model. The difference between the observed and the model field at each point of the grid, which we will refer to as ΔB, is a measure of the sum of the induced day magnetic field and the possible displacement of the crustal field lines. The radial magnetic field component, Br, was chosen for this approach, as it is less affected by external fields (Arkani-Hamed, 2004), providing the steadiest and least noisy data.

For the modeled field, we use the model developed by Morschhauser et al. (2014), which is a best fit of the observed lithospheric magnetic field of Mars, represented by an expansion of spherical harmonic functions up to degree and order 110. We chose this model because it has the highest spatial resolution among Martian crustal magnetic field models and it encompasses the whole MGS data set.

3.1.1. MAVEN Data Analysis

MAVEN data were selected for dawn and dusk regions only. As illustrated in Figure 1, dawn data cover the region between 04:00 LT and 12:00 LT, while dusk data lie between 12:00 LT and 20:00 LT. The median of the data every 4 seconds is displayed on grids of IAU (International Astronomical Union) areographic coordinates, with latitude and longitude bin-sizes of 0.5°. Each bin contains between 3 and 10 data points. Because the number of data points per bin is small, the external field contributions are not completely averaged out. However, we consider that these contributions do not affect the movement of the field lines, but only its magnitude. At an altitude range of 200-400 km, for example, the strongest values of the external field are in the order of ~40 nT, above areas of intense magnetic field, which corresponds to

~15% of the observed magnitude. We disregard further effects caused by the external induced field for our next analysis.

We plotted Br for the crustal model, dawn-side and dusk-side magnetic fields, each in four ranges of altitude, every 200 km between 200-1000 km. Figure 2 shows an example of these maps at dawn-side and dusk-side, between 200-400 km.

In order to better understand the magnitude and direction of the flow over crustal magnetic field structures, arrows representing the average direction and magnitude of horizontal velocity of ions were calculated with bin-size of 5°. We considered only the species of the ionospheric plasma which dominates the mass flux at this altitude, which is O_2^+ (Benna et al., 2015). The ion velocity vectors are obtained from an average over all observations by the MAVEN STATIC instrument between 1st December 2014 and 14th May 2018 in the altitude range of 200-400 km and energy range of 0-30 eV. Velocities have been corrected for spacecraft velocity and potential. The vector orientation is defined through the azimuthal and polar vector components in areographic coordinates. The vector length represents the magnitude where longest vectors have a magnitude of 3 km/s.

For a better visualization, Figure 2 shows those results with bin-size of 1° for the magnetic field and 15° for the velocity vectors. The blue and the red hatched bins represent values which are below the minimum value and above the maximum value of the color scale, respectively.

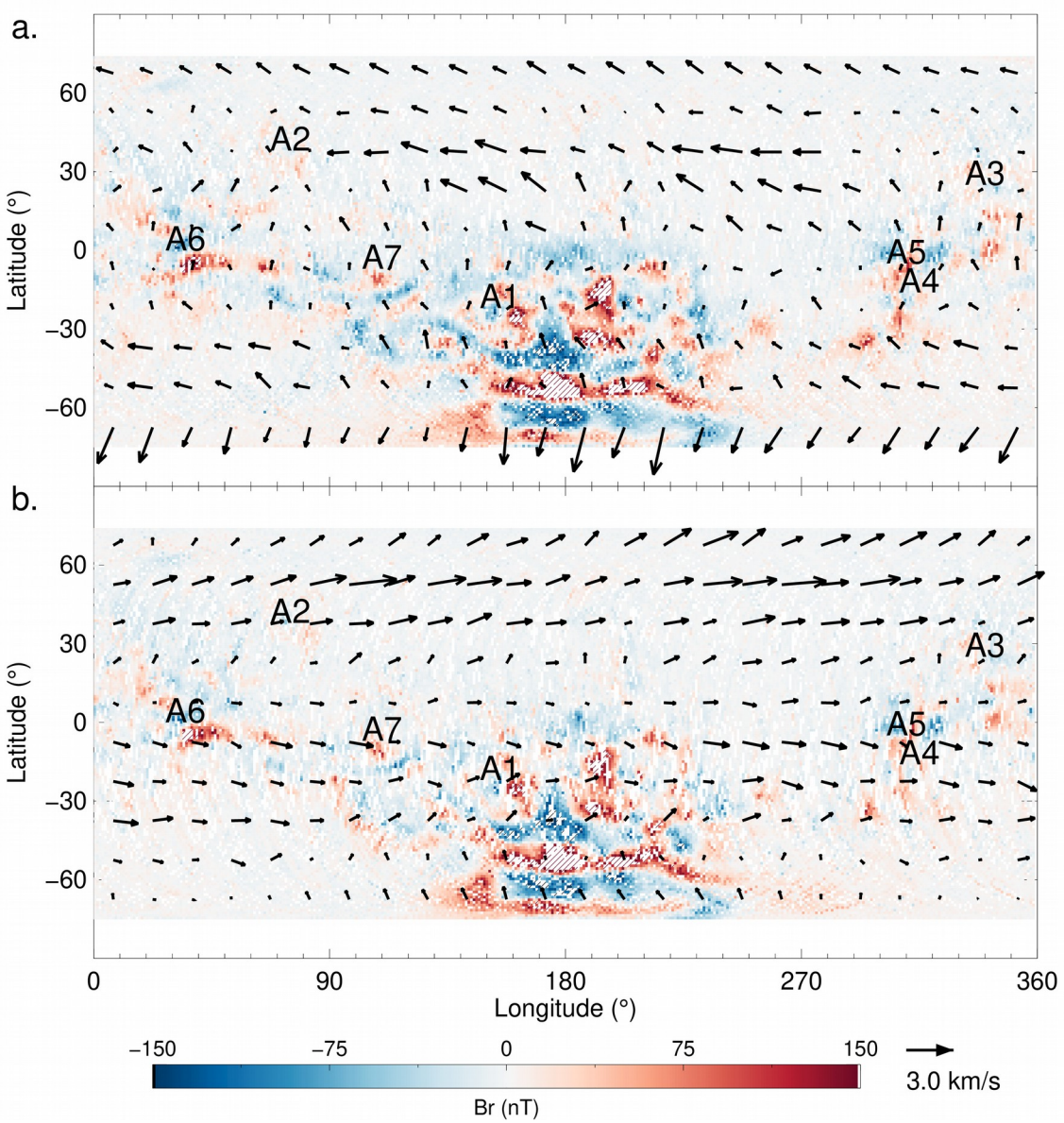

Figure 2. Maps of the radial component of the magnetic field obtained by MAVEN, at 200-400 km range, overplotted by arrows of O_2^+ horizontal velocity, at dawn-side (a) and dusk-side (b). A1-A7 correspond to the anomalous regions selected for MGS data analysis.

We first investigated whether there is a shift between observations and model on a global scale. Each crustal model grid was shifted between -5.0° (westward) and +5.0° (eastward), with steps of 0.5°, in the longitudinal direction, and a new parameter ΔB_{MAVEN} was calculated, where j is the number of points in the grid, as:

$$\Delta B_{MAVEN} = \frac{1}{j}\sum_{i=1}^{j} |Model\ Br_i - Observed\ Br_i| \quad (3)$$

If advection is present, a minimum value of ΔB_{MAVEN} is expected at some shift value. This optimum ΔB_{MAVEN} should be coherent with the direction of dragging of the magnetic field.

Table 1 presents the minimum ΔB_{MAVEN} values for each altitude range. The errors were estimated by calculating the average deviation of ΔB_{MAVEN} values from a fitted Gaussian function, with a confidence interval of 95%. As we see from the table, we only observe a shift value different from 0.0° for the high altitude dusk side observations.

Table 1. Minimum ΔB_{MAVEN} and their respective shift values, according to the altitude range.

Altitude (km)	**Min ΔB_{MAVEN} Shift Value (Dawn)**	**Min ΔB_{MAVEN} Shift Value (Dusk)**
200-400	0.0° ± 0.5°	0.0° ± 0.5°
400-600	0.0° ± 1.0°	0.0° ± 0.5°
600-800	0.0° ± 1.0°	0.0° ± 3.5°
800-1000	0.0° ± 3.5°	2.0° ± 1.5°

3.1.2. MGS Data Analysis

Since the results on global scale were not conclusive, we also did a higher resolution analysis, using MGS data. The crustal model developed by Morschhauser et al. (2014) is based on MGS data. In order to prevent misleading results due to the way the model was built, we decided to directly compare day-side (~02:00 LT) to night-side (~14:00 LT) observational data. We calculate ΔB_{MGS} as:

$$\Delta B_{MGS} = \frac{1}{j}\sum_{i=1}^{j} |Nighttime\,Br_i - Daytime\,Br_i| \quad (4)$$

As for low latitudes an azimuthal motion is expected, we made grids with latitude and longitude bin-sizes of 1.0^o and 0.1^o, respectively, also averaged every 4 seconds. In each bin, there are between 20 and 80 data points, which means that external field contributions are averaged out in this analysis. MGS data present a strong orbital bias, so a latitudinal smoothing was performed for every 10 bins. The technique was applied for a global map and for selected magnetic anomalous regions, indicated by the labels A1-A7 in Figure 2. An example of the maps at day-side and night-side data for anomalies A2, A4 and A6 is shown in Figure 3.

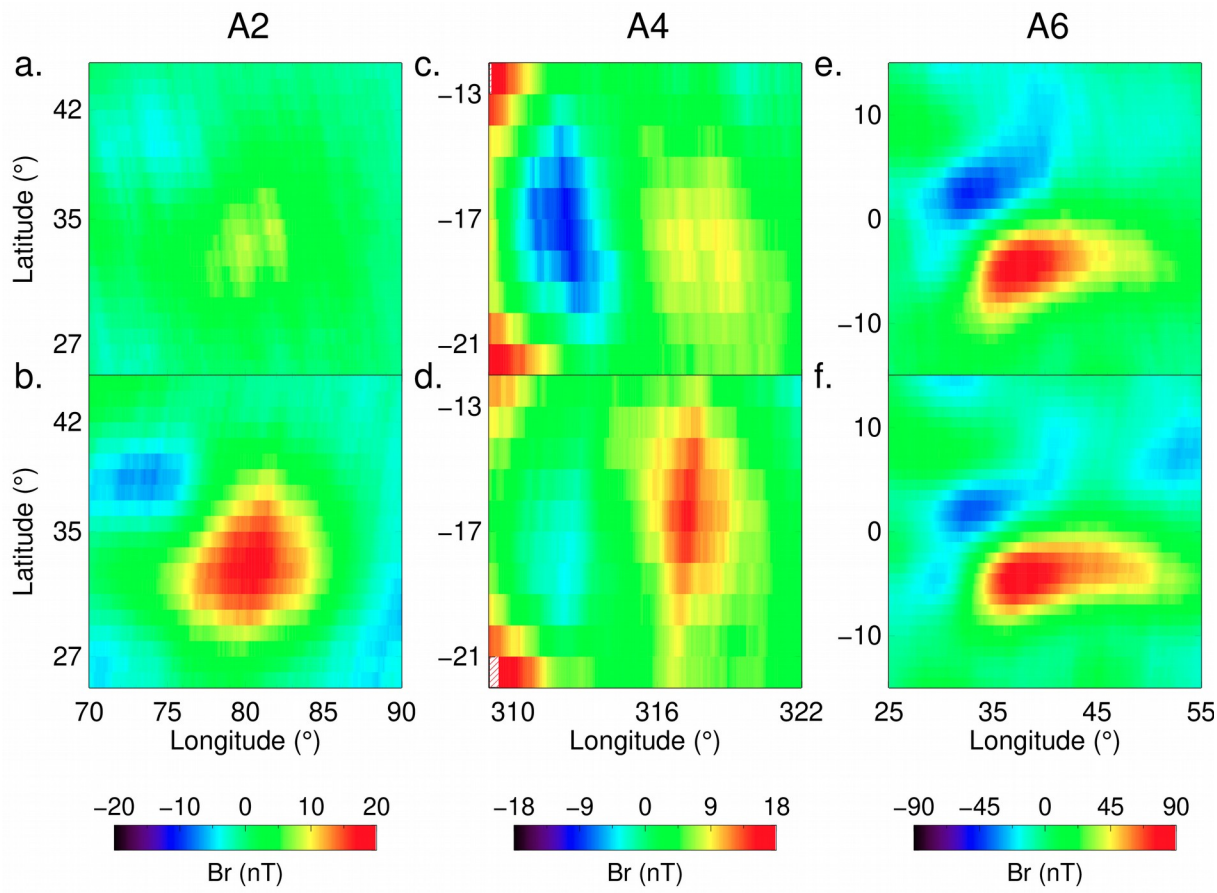

Figure 3. Maps of the radial component of the magnetic field obtained by MGS, for A2 at day-side (a) and night-side (b), for A4 at day-side (c) and night-side (d) and for A6 at day-side (e) and night-side (f).

Nighttime grids were shifted in longitudinal steps of 0.1°, between -1.0° and +1.0°. Table 2 presents the shift value of the lowest ΔB_{MGS} for each grid, and the respective errors.

Table 2. Minimum ΔB_{MGS} and their respective shift values.

Position	**Min ΔB_{MGS} Shift Value**
Global Map	-0.1° ± 0.4°
A1	0.0° ± 0.3°
A2	0.8° ± 0.4°
A3	1.0° ± 0.3°

A4	0.3° ± 0.3°
A5	-0.1° ± 0.4°
A6	-0.5° ± 0.3°
A7	0.3° ± 0.3°

As we see from Table 2, for regions A2 and A3 in the Northern hemisphere a significant shift is observed. This allows us to calculate the possible advection speed of the crustal magnetic field lines. We consider an altitude of 400 km, a planetary radius of 3393.5 km, a minimum shift of 0.1° and a maximum of 1.0°, and take into account that the ionospheric flow has acted on the crustal field lines over a period of up to 2 hours at the point of observation (between noon and 14:00 local time limited by the MGS daytime coverage). The co-rotation speed of the magnetic field lines at this altitude is about 0.26 km/s – significantly lower than the ionospheric day-to-night flow speed of about 1-2 km/s. A shift of the field line by 1.0° corresponds to a distance of 66 km at this altitude. If we assume that this shift is caused by the action of the plasma flow over 1 hour, we can derive an advection velocity of about 18 m/s at this location.

3.2. Analysis of Pressures

In general, the advection of magnetic fields in a moving plasma is a complicated problem because it is influenced by conductivity and magnetic diffusion (see Lui, 2018, and Wilmot-Smith et al., 2005, for a general discussion of the problem). In the Martian ionosphere, conductivity and magnetic diffusion change significantly with altitude and are difficult to deduce from observations. But to get a general idea of the relative forces between the moving plasma and the crustal fields, we consider in this paragraph the pressures involved in the advection process.

The dynamic pressure of the ionospheric plasma flow, where ρ is the mass density and v is the horizontal speed of the flow, is given by Equation 4. For this calculation, we used the measurements of O_2^+ ions.

$$p_{Dyn} = \frac{\rho v^2}{2} \tag{4}$$

The magnetic pressure of the field lines, where B is the magnetic field intensity, is given by Equation 5. Only the crustal magnetic field model was considered, as our aim is to investigate the mini-magnetosphere structures solely.

$$p_{Mag} = \frac{\boldsymbol{B}^2}{2\mu_0} \tag{5}$$

The thermal pressure of the plasma, where n is the number density and T is the temperature of ions and electrons related to the mini-magnetospheres, is given by Equation 6. The ion moments were calculated from the distribution functions measured by the MAVEN STATIC instrument and corrected for spacecraft potential and spacecraft velocity (Dubinin et al., 2017).

$$p_{Th} = K_B \left(n_e T_e + n_i T_i \right) \tag{6}$$

For this method, MAVEN data were used. The data were sorted according to the magnetic field intensity. At a height of 400 km, we define “low intensity crustal magnetic field” (LF) when the absolute value of the magnetic field component is below 10 nT, and “high intensity crustal magnetic field” (HF) when this value is above 10 nT.

We created local time vs. altitude grids for the data, with bin-sizes of 30 min and 20 km, respectively, using 4 seconds resolution data. Plots for O_2^+ density and horizontal speed and the calculated pressures for regions of low and high intensity crustal magnetic field are shown in Figures 4 and 5. The black and the red hatched bins represent values which are below the minimum value and above the maximum value of the color scale, respectively.

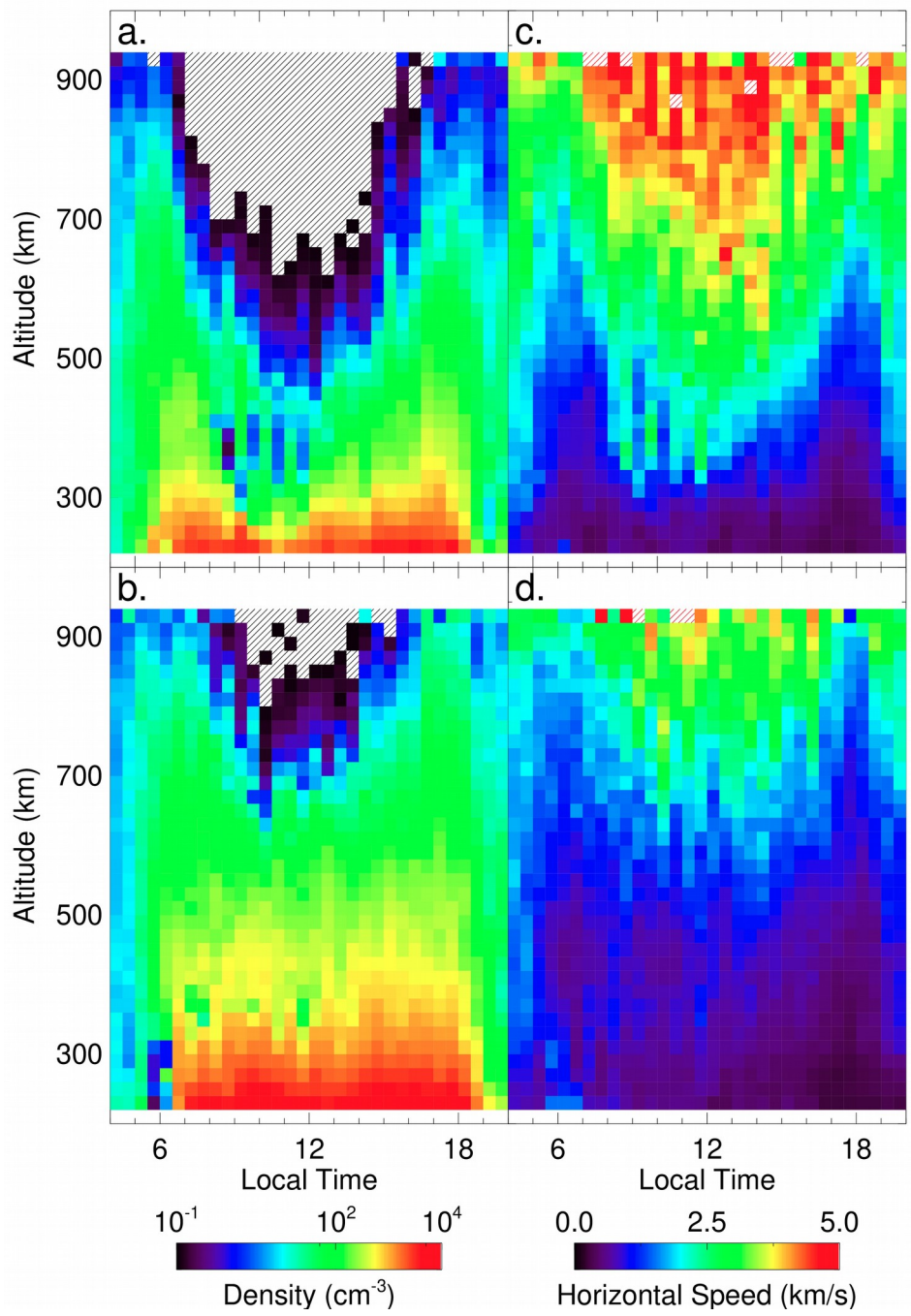

Figure 4. Local time vs. altitude plots for O_2^+ density above LF (a) and HF regions (b) and for O_2^+ horizontal speed above LF (c) and HF regions (d).

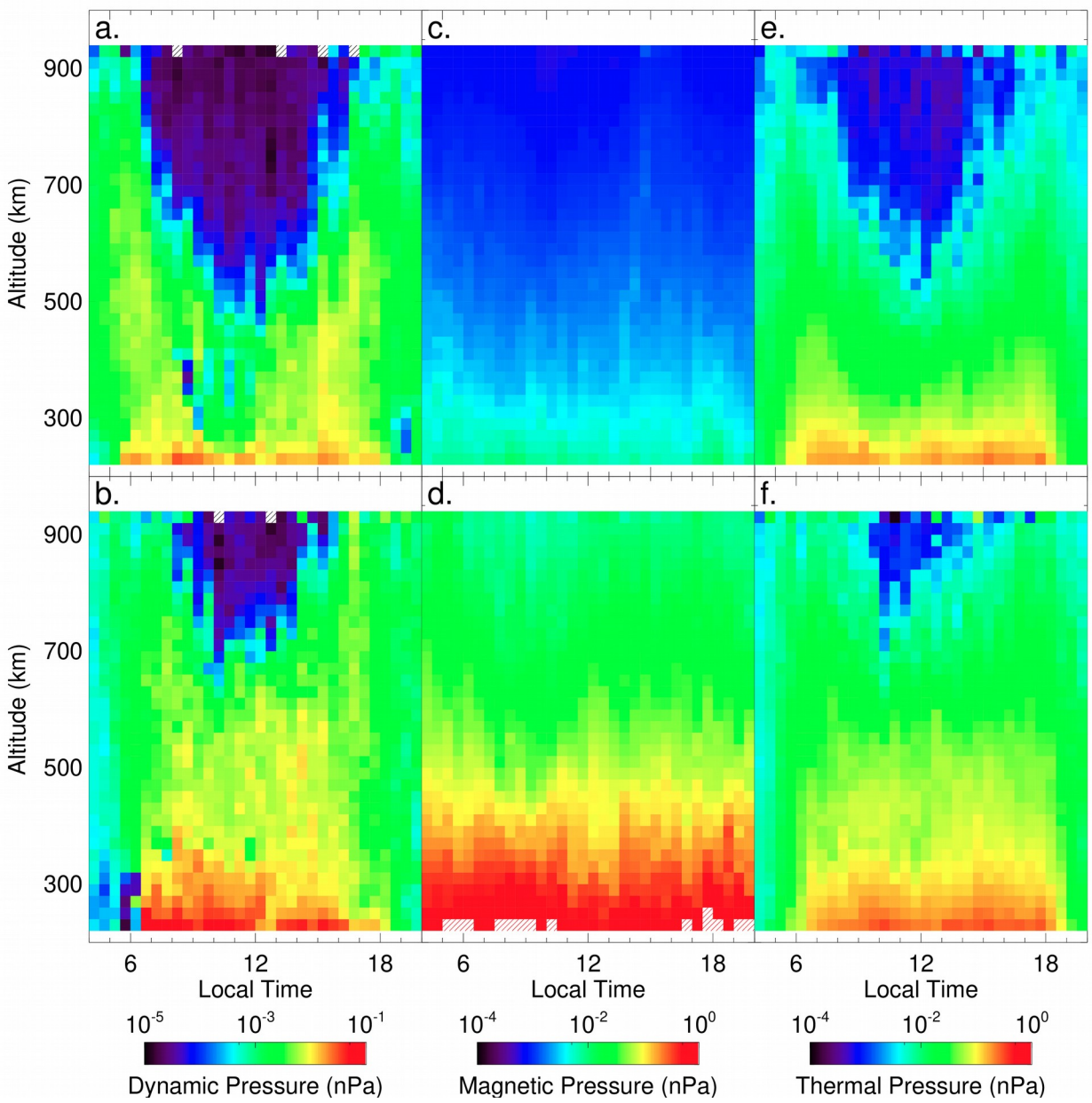

Figure 5. Local time vs. altitude plots of the pressures for both regions of low and high intensity crustal magnetic fields. Dynamic pressure for LF (a) and HF (b) regions. Magnetic pressure for LF (c) and HF (d) regions. Thermal pressure for LF (e) and HF (f) regions. Note the different color scale ranges.

In regions where the plasma dynamic pressure is higher than the sum of magnetic and thermal pressures, we should expect that vertical magnetic structures are always moved by the momentum imposed by the plasma flow. But advection of the field is a diffusive process which can also occur at lower dynamic pressure. Another condition for the occurrence of advection is a high, but finite, conductivity of the ionospheric plasma. In order to analyze the pressure balance,

we calculated the following ratio for regions of low and high intensity crustal magnetic field, shown in Figure 6:

$$ratio = \frac{p_{Dyn}}{p_{Mag} + p_{Th}} \tag{7}$$

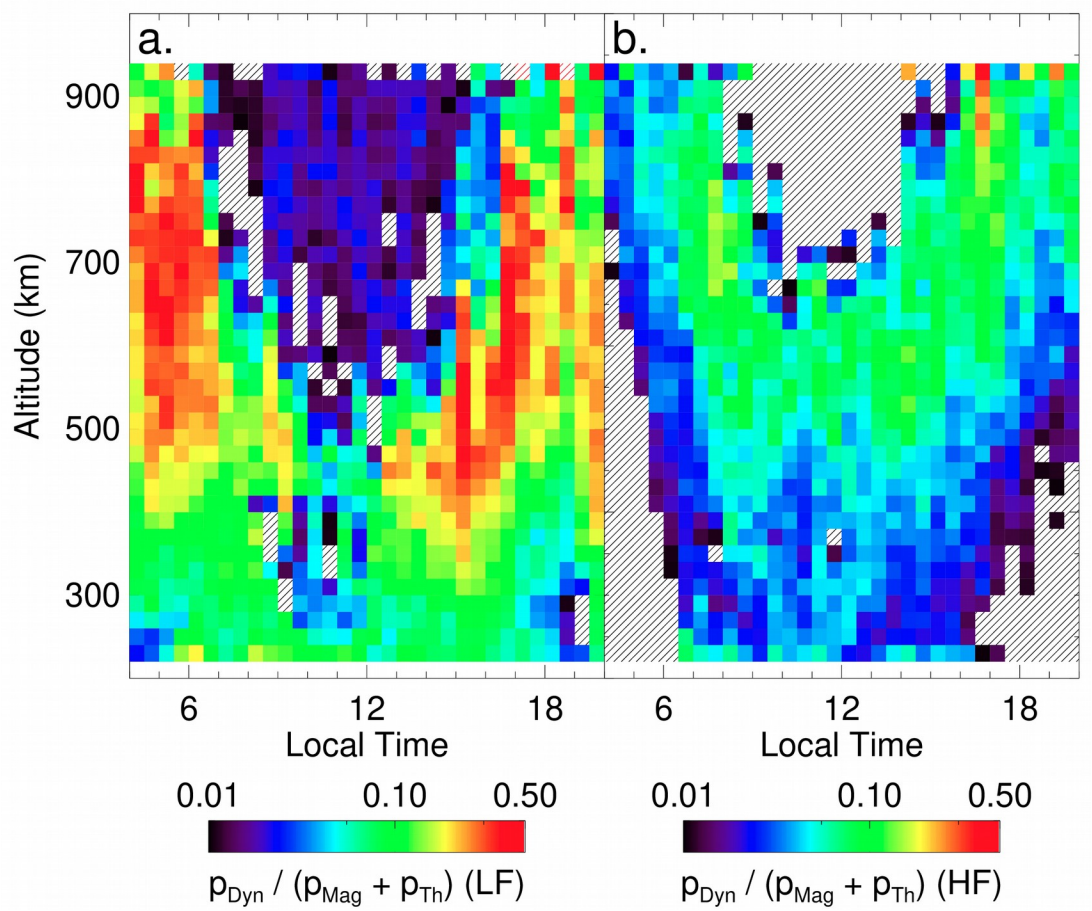

Figure 6. Local time vs. altitude plots of the pressure ratio for regions of low (a) and high (b) intensity crustal magnetic fields.

4 Discussion

In this section, the results obtained by the two applied techniques are discussed and related to the advection process.

In the global grids made with MAVEN data, as in Figure 2, we observe that the magnetic field at dawn- and dusk-side are slightly distinct in shape and in magnitude, especially above areas of strong magnetic field. Some explanations for dawn/dusk asymmetries are the influence of the interplanetary magnetic field direction (e.g. Walsh et al., 2012), counterclockwise rotation and translation motions of the planet, which create greater pressure on the dawn-side, the small number of data points per bin in our grids or the advection effect.

Figure 2 also shows that O_2^+ horizontal speed is greater above areas where the crustal magnetic fields are weak – namely in the Northern hemisphere. Above strong magnetic fields, the plasma flow is irregular and has no preferred direction. Because this is a statistical analysis, most of the vectors cancel each other, and the final result shows that the speed above strong fields is low, on average.

The results presented in Table 1 show that, for the majority of the cases, ΔB_{MAVEN} is minimum when there is no shift and the errors are large. This could either mean that advection does not frequently occur or that MAVEN data coverage is not yet sufficient for analyzing subtle changes in the magnetic field.

The results regarding MGS data, shown in Figure 3, present differences between day-side and night-side regions with respect to the shape and the magnitude of magnetic field. However, there is no clear pattern of displacement of the magnetic field regions. For example, A2 presents weaker fields during the day, while A4 has an increase in the negative fields and A6 seems to have its shape contracted during the same period.

The results in Table 2 confirm the lack of pattern, as the shift values for minimum ΔB_{MGS} are, mostly, very small and with no preferred direction. The exceptions are anomalies A2 and A3, with higher values of shift. Both of them are located in the Northern hemisphere, at mid latitudes and further away from the other selected anomalies. The ionospheric plasma flow above those regions is less perturbed than above regions of intense magnetic fields and this could be the reason we observe larger values of shift, which are oriented eastward, as it was expected for advection at dawn-side regions.

MGS analysis results are restricted with respect to altitude and local time ranges, which leads to a limited analysis in these aspects. The possible advection speed of motion of the crustal field lines is about 18 m/s at 400 km altitude, which is very slow when compared to the average horizontal plasma speed of 500-1000 m/s and the co-rotational speed of 275 m/s.

From Figure 4, we observe that the horizontal speed and the density of O_2^+ ions are inversely, but not linearly, related. The horizontal speed increases while the density decreases as a function of altitude, for both low and high magnetic field regions. Although the O_2^+ horizontal speed is smaller above areas of high intensity magnetic fields, the ion density above those regions is large enough to produce a more significant dynamic pressure there than above low intensity fields, like shown in Figure 5. However, thermal pressure is, on average, larger than dynamic pressure, on both regions. This means that, even if we were not considering magnetic pressure in the balance, dynamic pressure alone would not be enough for the ionospheric flow to break the stability of the magnetic field lines.

According to the results shown in Figure 6, the highest values of the pressure ratio occur at medium to high altitudes above regions of low intensity fields, at the terminators of the planet. Considering the altitude, the intensity of the field and the value of the ratio (~0.5), a displacement of the magnetic field cannot be simply explained by dynamic pressure alone. In fact, the observed displacement needs to be explained by a diffusive process, like advection.

5 Conclusions and Future Prospects

In this work, we propose the hypothesis that the ionospheric plasma flow in Mars could transport crustal magnetic field lines in the day-to-night direction. To study the existence of that

phenomenon, two types of statistical analyses were made using data from the spacecrafts MGS and MAVEN.

First, we directly compared areographic coordinates grids of observed MAVEN data and modeled magnetic field, shifting the latter in longitude, in order to investigate if there was an optimum offset where the difference between them was minimum. We did the same type of analysis with MGS data, comparing nighttime and daytime data. Most of the results showed that this difference was minimum when there is no offset, except for regions of mid latitudes at the Northern hemisphere. Although we can clearly observe differences between day-side and night-side data from the MGS grids, this behavior cannot be explained by a simple subtraction, as we propose in this work.

Next, we analyzed how large is the dynamic pressure of the ionosphere when compared to magnetic and thermal pressures of the crustal magnetic structures. The effect of the crustal magnetic fields on the ionosphere flow is more present than the opposite way. The plasma flow cannot break the stability of the magnetic field structures, in average. For that reason, it might not be possible to spot evidence of advection by a global statistical analysis.

In conclusion, using MAVEN and MGS databases, we did find some evidence of Mars' crustal field displacement due to advection by the ionospheric plasma flow for weak anomalies in Northern hemisphere. The reasons for this effect being difficult to detect is that the advection velocity is very slow (~18 m/s) as compared to the co-rotation speed.

Investigating single orbits data where the displacement of the magnetic field can be directly observed could be a more reliable, although time consuming, way to approach the problem. Therefore, in a future work, regions of isolated magnetic anomalies in the Northern hemisphere should be the focus of analysis. Finally, we also plan to model the advection in a magneto-hydrodynamic model using the plasma conditions prevalent in the Martian ionosphere.

Acknowledgments and Data Availability Statement

We would like to thank the Max-Planck-Institute for Solar System Research for the facilities, data provision and collaboration. The maps and plots of this article were produced with the CCATi software (http://www2.mps.mpg.de/projects/mars-express/aspera/ccati/). The work was funded by the São Paulo Research Foundation (under grants 2016/10794-2, 2017/00516-8, 2018/17098-7, 2018/216557-1 and 2019/01716-6) and by the Brazilian National Council for Scientific and Technological Development (under grants 131260/2018-9, 300234/2019-8, 301883/2019-0 and PQ-302583/2015-7). The data processing at the Max-Planck-Institute was supported by the German Space Agency under grant 50QM1703. MGS and MAVEN data are available at the NASA Planetary Plasma Interactions Node (https://pds-ppi.igpp.ucla.edu/). We would like to acknowledge Jack Connerney and Jim McFadden for providing the data used in this work.

References

M. H. Acuña, J. E. P. Connerney , P. Wasilewski, R. P. Lin, K. A. Anderson, C. W. Carlson, et al. (1992). Mars Observer magnetic fields investigation, *J. Geophys. Res.*, 97 (E5), 7799 – 7814. https://doi.org/10.1029/92JE00344

M. H. Acuña, J. E. P. Connerney, P. Wasilewski, R. P. Lin, K. A. Anderson, C. W. Carlson, et al. (1998). Magnetic Field and Plasma Observations at Mars: Initial Results of the Mars Global Surveyor Mission, *Science, 279* (5357), 1676 – 1680. https://doi.org/science.279.5357.1676

Albee, A. L., Arvidson, R. E., Palluconi, F., and Thorpe, T. (2001). Overview of the Mars Global Surveyor mission, *J. Geophys. Res., 106* (E10), 23291 – 23316. https://doi.org/10.1029/2000JE001306

Andersson, L, Ergun, R. E., Delory, G. T., Eriksson, A., Westfall, J., Reed, H., et al. (2015). The Langmuir Probe and Waves (LPW) Instrument for MAVEN, *Space Sci. Rev., 195* (1-4), 173 – 198. https://doi.org/10.1007/s11214-015-0194-3

Arkani-Hamed, J. (2004). A coherent model of the crustal magnetic field of Mars, *J. Geophys. Res., 109* (E09005). https://doi.org/10.1029/2004JE002265

Benna, M., Mahaffy, P. R., Gebrowsky, J. M., Fox, J. L., Yelle, R. V., Jakosky, B. M. (2015). First measurements of composition and dynamics of the Martian ionosphere by MAVEN's Neutral Gas and Ion Mass Spectrometer, *Geophys. Res. Lett., 42* (21), 8958 – 8965. https://doi.org/10.1002/2015GL066146

Bittencourt, J. A. (1995). *Fundamentals of Plasma Physics* (2nd Ed), São José dos Campos: J. A. Bittencourt/FAPESP

Brain, D. A. (2006). Mars Global Surveyor Measurements of the Martian Solar Wind Interaction, *Space Science Reviews, 126* (1-4), 77 – 112. https://doi.org/10.1007/s11214-006-9122-x

Brain, D. A., Bagenal, F., Acuña, M. H., Connerney, J. E. P. (2003). Martian magnetic morphology: Contributions from the solar wind and crust, *J. Geophys. Res., 108* (A12), https://doi.org/10.1029/2002JA009482

Brain, D. A., Baker, A. H., Briggs, J., Eastwood, J. P., Halekas, J. S., Phan, T. -D. (2010). Episodic detachment of Martian crustal magnetic fields leading to bulk atmospheric plasma escape, *Geophys. Res. Lett., 37* (L14108), https://doi.org/0.1029/2010GL043916

Connerney, J. E. P., Espley, J., Lawton, P., Murphy, S., Odom, J., Oliversen, R., Sheppard, D. (2015). The MAVEN Magnetic Field Investigation, *Space Sci. Rev., 195* (1-4), 257 – 291. https://doi.org/10.1007/s11214-015-0169-4

Dubinin, E., Fraenz, M., Pätzold, M., McFadden, J., Mahaffy, P. R., Eparvier, F. (2017). Effects of solar irradiance on the upper ionosphere and oxygen ion escape at Mars: MAVEN observations, *J. Geophys. Res.: Space Phys., 122* (7), 7142 – 7152. https://doi.org/10.1002/2017JA024126

Gresho, P.M., & Sani, R.L. (2000). Incompressible Flow and the Finite Element Method: Advection-Diffusion. (Vol. 1). United States: John Wiley and Sons.

Jakosky, B. M., Lin, R. P., Grebowsky, J. M., Luhmann, J. G., Mitchell, D. F. (2015). The Mars Atmosphere and Volatile Evolution (MAVEN) Mission, *Space Sci. Rev., 195* (1-4), 3 – 48. https://doi.org/10.1007/s11214-015-0139-x

Luhmann, J. G., Russel, C. T., Brace, L. H., Vaisberg, O. L. (1992). The Intrinsic Magnetic Field and Solar-Wind Interaction of Mars. In G. Michael (Ed.), *Mars* (1090 – 1134), North Mankato, MN: The Child's World Inc.

Lui, A.T.Y. (2018). Frozen-in condition for ions and electrons: implication on magnetic flux transport by dipolarizing flux bundles. *Geosci. Lett. 5* (5). https://doi.org/10.1186/s40562-018-0104-0

Ma, Y., Nagy, A. F., Hansen, K. C., Dezeeuw, D. L., Gombosi, T. I., Powell, K. G. (2002). Three-dimensional multispecies MHD studies of the solar wind interaction with Mars in the presence of crustal fields, *J. Geophys. Res.: Space Phys., 107* (A10), https://doi.org/10.1029/2002JA009293

McFadden, J. P., Kortmann, O., Curtis, D., Dalton, G., Johnson, G., Abiad, R. (2015). MAVEN SupraThermal and Thermal Ion Compostion (STATIC) Instrument, *Space Sci. Rev., 195* (1-4), 199 – 256. https://doi.org/10.1007/s11214-015-0175-6

Mitchell, D. L., Lin, R. P., Mazelle, C., Rème, H., Cloutier, P. A., Connerney, J. E. P., Acuña, M. H., Ness, N. F. (2001). Probing Mars' crustal magnetic field and ionosphere with the MGS Electron Reflectometer, *J. Geophys. Res., 107* (E10), 23419 – 23428. https://doi.org/10.1029/2000JE001435

Morschhauser, A., Lesur, V., Grott, M. (2014). A spherical harmonic model of the lithospheric magnetic field of Mars, *J. Geophys. Res.: Plan.*, *119* (6), 1162 – 1188. https://doi.org/10.1002/2013JE004555

Podgorny, I. M., Dubinin, E. M., Israelevich, P. L. (1980). Laboratory Simulation of the Induced Magnetospheres of Comets and Venus, *Moon and Plan.*, *23* (3), 323 – 338. https://doi.org/10.1007/BF00902047

Walsh, B. M., Sibeck, D. G., Wang, Y., Fairfield, D. H. (2012). Dawn-dusk asymmetries in the Earth's magnetosheath, *J. Geophys. Res.: Space Phys.*, *117* (A12). https://doi.org/10.1029/2012JA018240

Wilmot-Smith, A. L., Priest, E. R., Hornig, G. (2005). Magnetic diffusion and the motion of field lines, *Geophys. Astrophys. Fluid Dyn.*, *99* (2), 177 – 197. https://doi.org/10.1080/03091920500044808